Supplementary Information (SI)

Roles Played by Carbene Substituents During Ligand Transfer Reactions Between Tungsten Fischer Carbene Complexes and [Pt(COD)Cl_2]

Nora-ann Weststrate[a], Christopher Hassenrück[b], David C. Liles[a], Simon Lotz[a], Helmar Görls[c], Rainer F. Winter[b]*

[a] *Department of Chemistry, University of Pretoria, Pretoria, 0002, South Africa, E-mail: simon.lotzup@gmail.com*

[b]*Fachbereich Chemie, Universität Konstanz, Konstanz, 78457, Germany, E-mail: rainer.winter@uni-konstanz.de*

[c]*Institut für Anorganische und Analytische Chemie, Friedrich-Schiller-Universität Jena, Jena, 07743, Germany*

Contents

IR spectroscopic identification of the counter ion present in complex 2b(I)

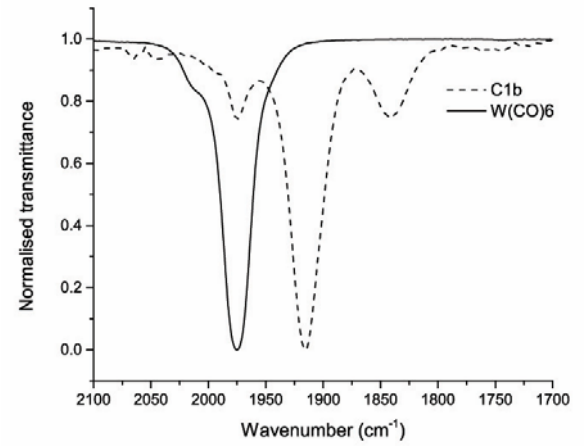

Figure S1. *FT-IR spectrum of* ***2b(I)*** *(····) and* $[W(CO)_6]^{(-)}$ *in* CH_2Cl_2 *at ambient temperature.*

Infrared spectroscopy played an important role in the identification of **2b(I)**. During its analysis, the presence of the tungsten carbonyl complex is observed in the ^{13}C NMR spectrum (S5). However, based on the structure refinement studies, the single X-Ray structure of the compound originally indicated that the compound was a charged tungsten hexacarbonyl species. It has been previously reported that it is possible for the wrong identification of elements from single X-Ray crystallography. By closer inspection it was clear that the error resulted from the fact that the crystallographic position of the chloro ligand at more than one of the carbonyl sites, diluting its effect. Hence IR spectroscopy was a key to clarify differences in ^{13}C NMR and X-ray crystallography data and the determination that the counter ion was in fact a $[W(CO)_5Cl]^-$ ion. The FT-IR spectrum of **2b(I)** against $W(CO)_6$ in CH_2Cl_2 is shown emphasizing the vast difference between the two compounds. The solid-state FT-IR spectrum for **2b(I)** shows three distinct peaks at 1988, 1893 and 1831 cm^{-1} (S1). For $W(CO)_6$ a single stretching frequency is expected at approximately 1980 cm^{-1}, thus eliminating the possibility that $W(CO)_6$ is present.[1] The solid state (KBr pellets) IR stretching frequencies of the tetraalkylammonium salts with the tungsten pentacarbonyl chloride anion are reported as three distinct peaks at 2061(w), 1904(s) and 1869(m) cm^{-1} for the A^1, E and A^2 stretching frequencies respectively.[2] Since the obtained IR spectrum closely matches the pattern as well as the approximate frequencies of vibration for the tetraalkylammonium tungsten pentacarbonyl chloride, it has been concluded that the anion of the **2b(I)** complex is the $[W(CO)_5Cl]^-$ ion.

NMR Spectroscopy

2a

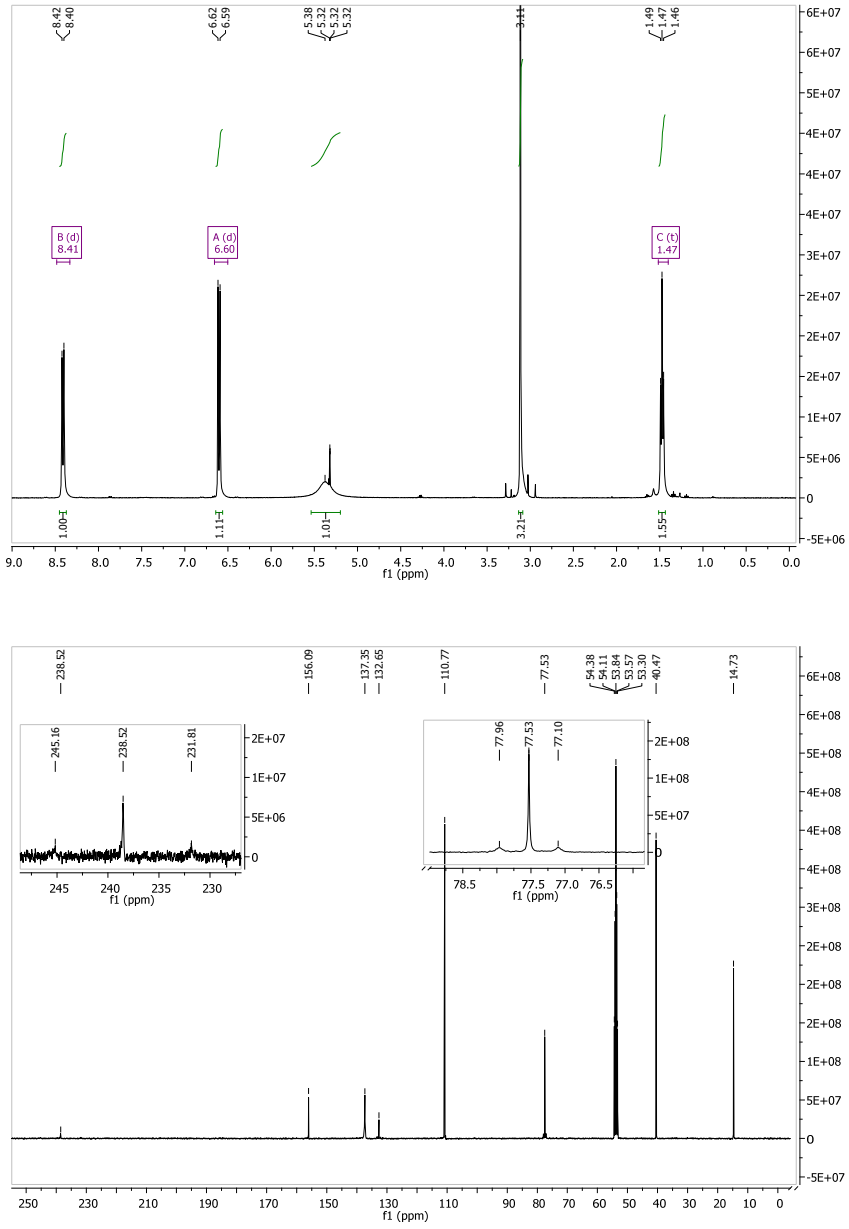

Figure S2. *^{1}H (top) and ^{13}C NMR (bottom) spectra of* ***2a*** *in CD_2Cl_2 at 298 K.*

4a

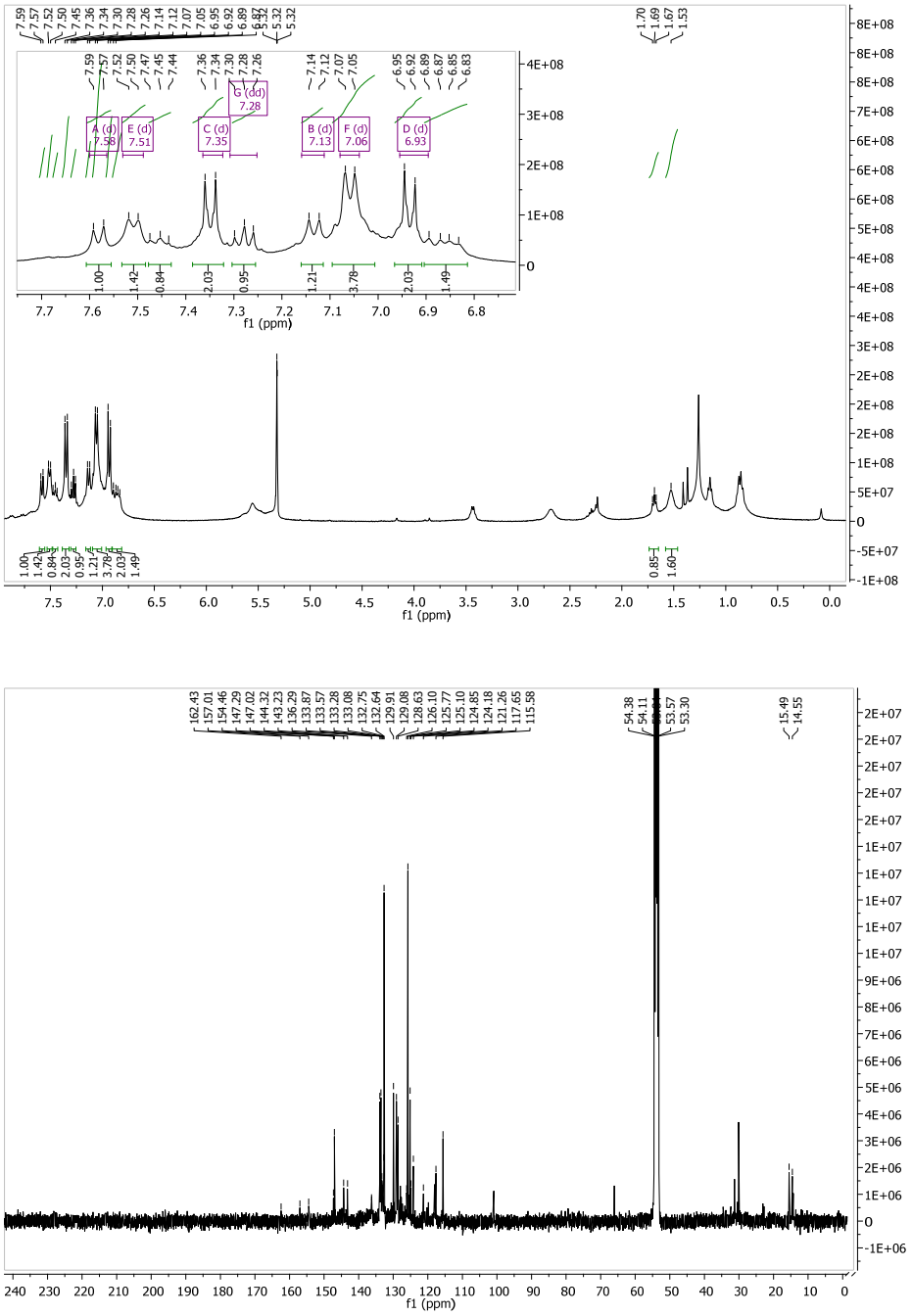

Figure S3. *^{1}H (top) and ^{13}C NMR (bottom) spectra of* ***4a*** *in CD_2Cl_2 at 298 K.*

1b

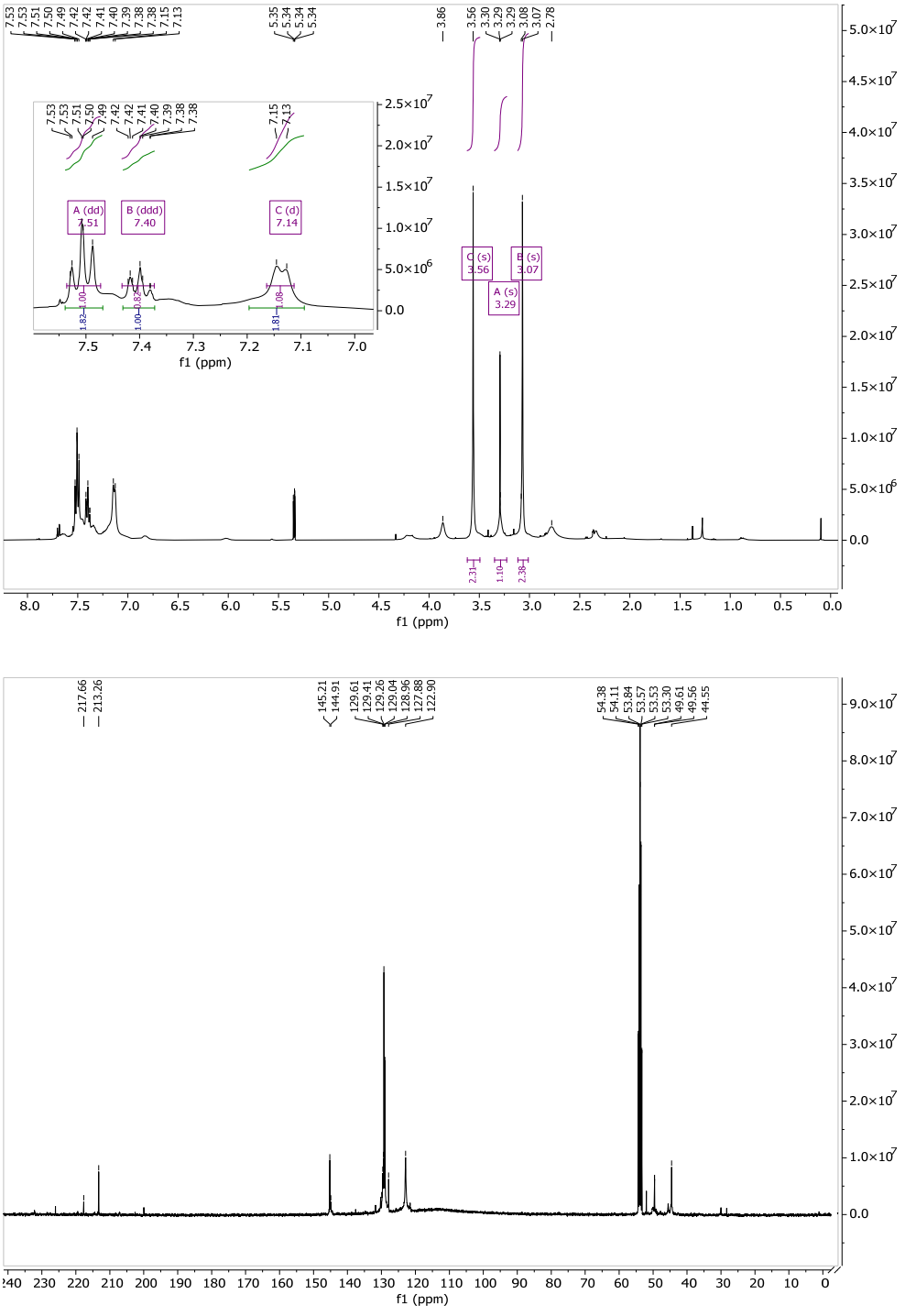

Figure S4. *[1]H (top) and [13]C NMR (bottom) spectra of* ***1b*** *in CD_2Cl_2 at 298 K.*

2b(I)

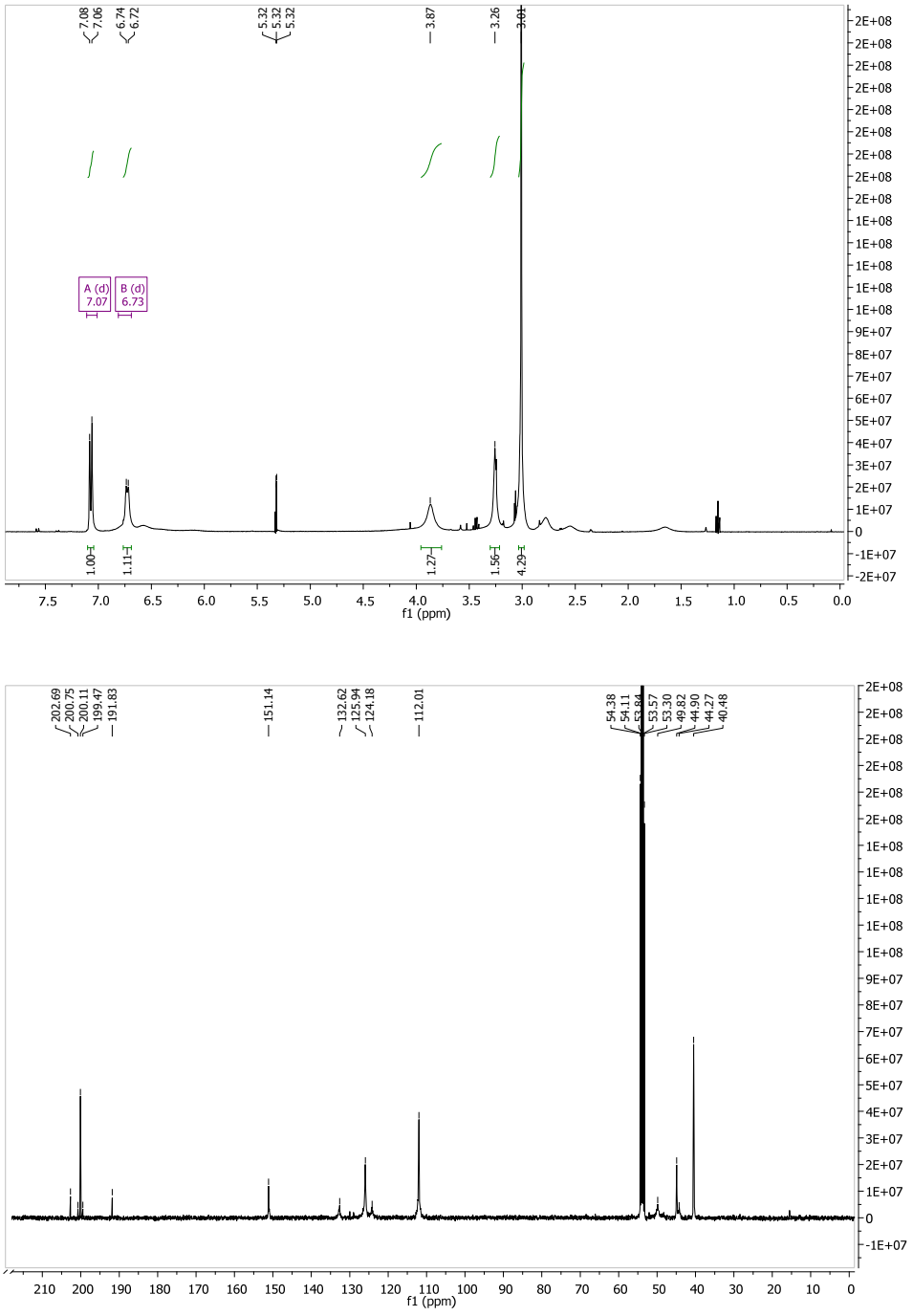

Figure S5. *^{1}H (top) and ^{13}C NMR (bottom) spectra of* ***2b(I)*** *in CD_2Cl_2 at 298 K.*

3b

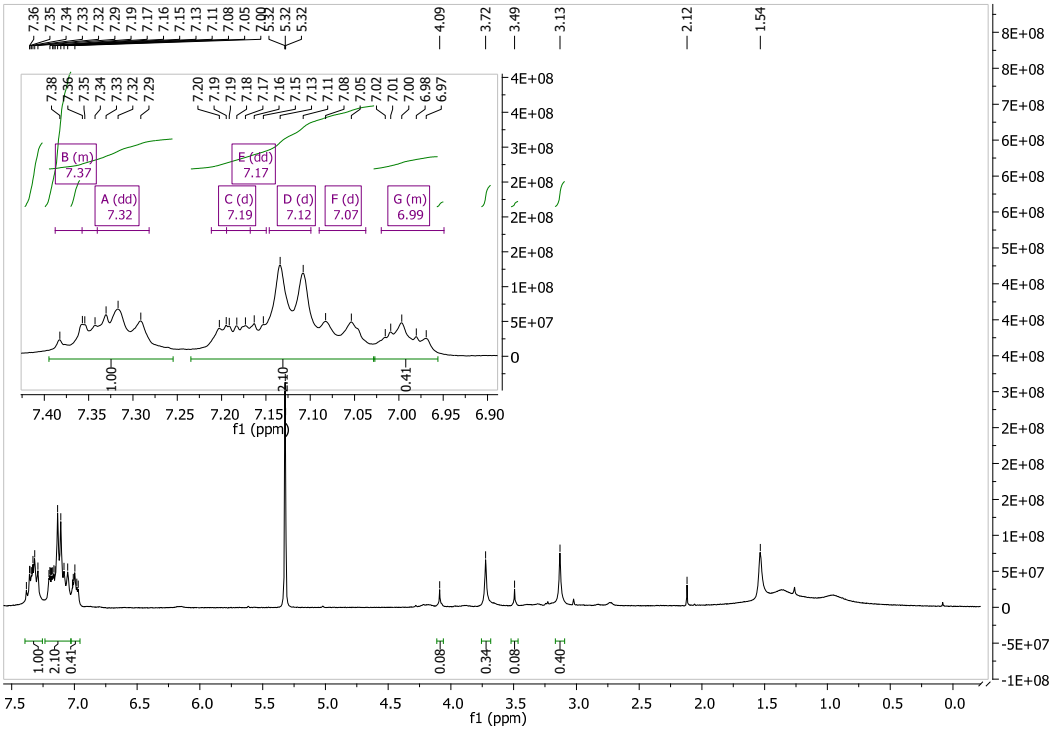

Figure S6. *^{1}H NMR spectra of* ***3b*** *in CD_2Cl_2 at 298 K.*

4b

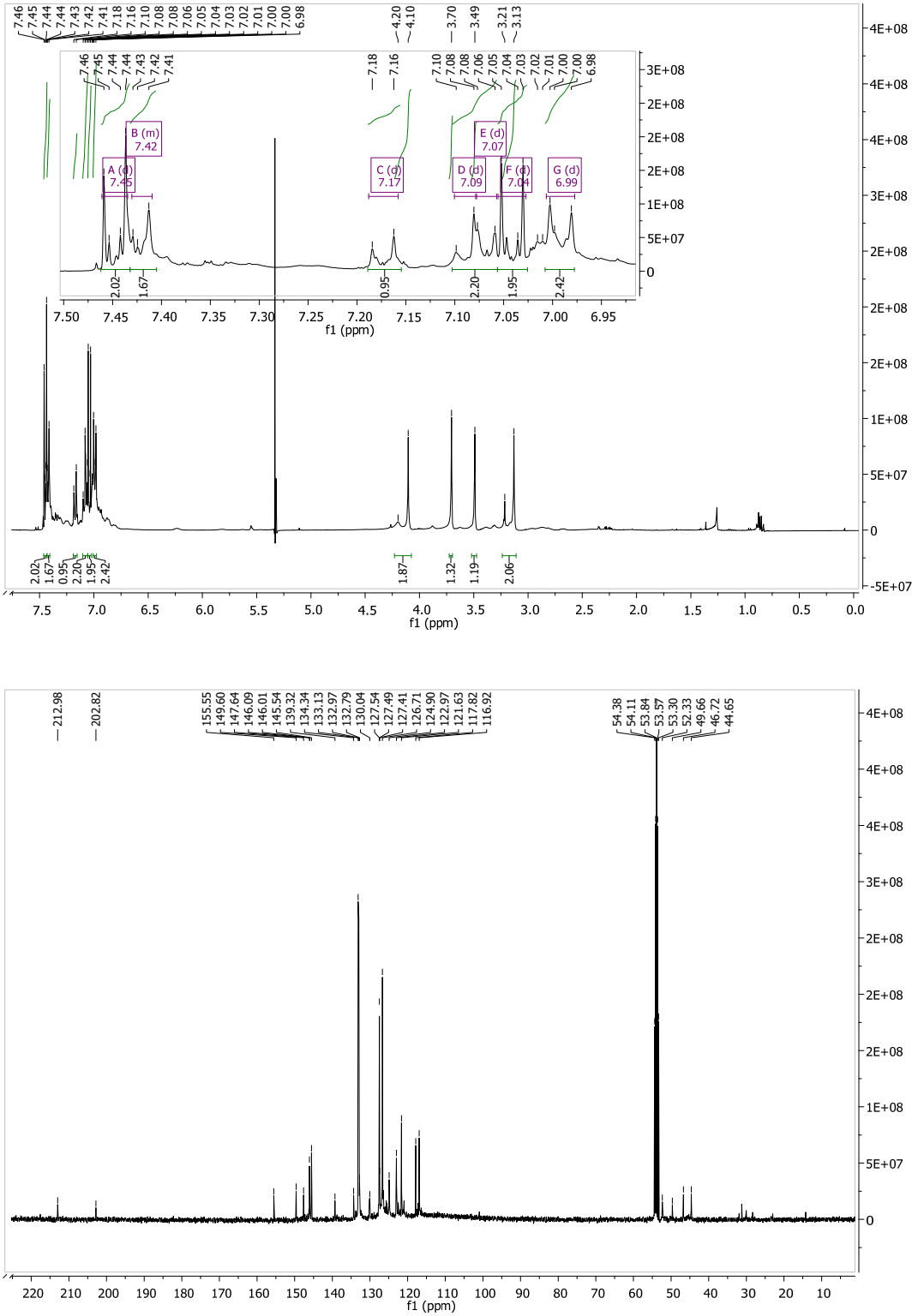

Figure S7. *^{1}H (top) and ^{13}C NMR (bottom) spectra of* ***4b*** *in CD_2Cl_2 at 298 K.*

High Resolution Mass Spectrometry

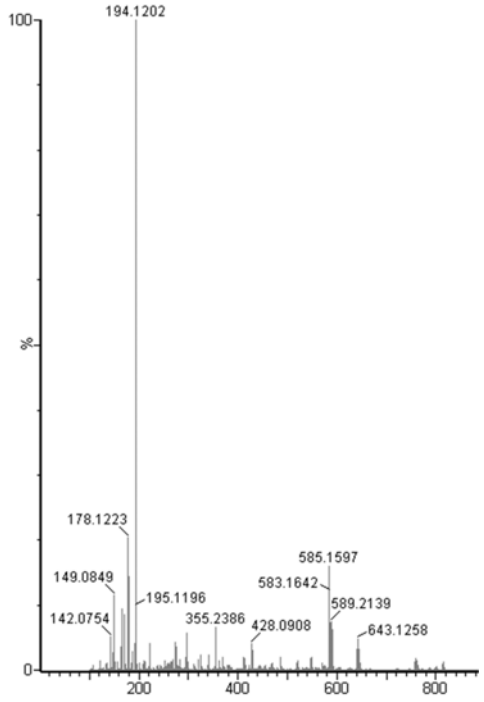

Figure S8. *ESI mass spectrum of* ***2a****.*

ESI-MS (2.8eV, positive mode, *m/z*): calcd for $[M + Na]^+$ 643.1263; found 643.1258.

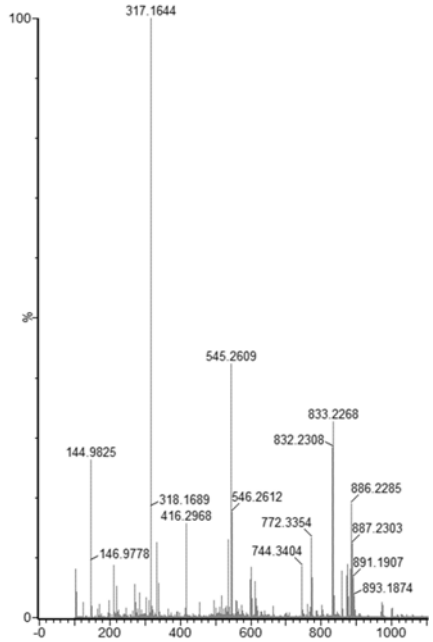

Figure S9. *ESI mass spectrum of* ***3a****.*

ESI-MS (2.8eV, positiv e mode, *m/z*): calcd for $[M - Cl]^+$ 833.2271; found 833.2268.

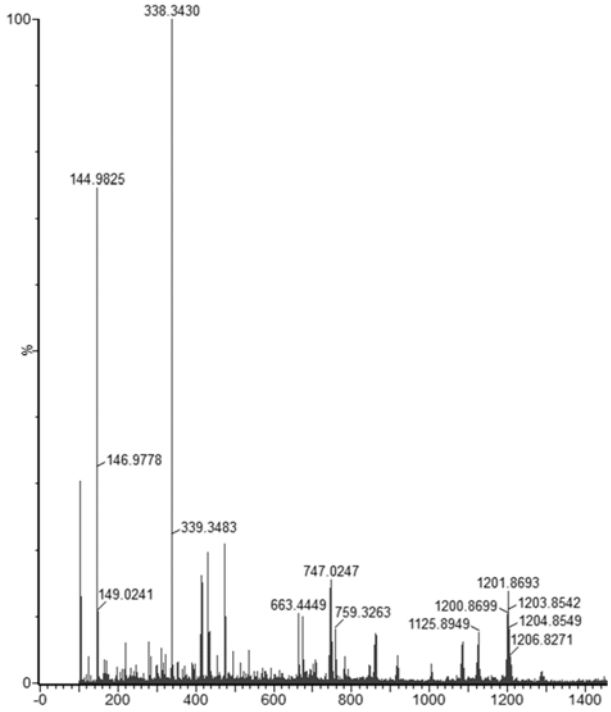

Figure S10. *ESI mass spectrum of* ***4a***

ESI-MS (2.8eV, positive mode, m/z): calcd for $[M + Na]^+$ 1206.8269; found 1206.8271.

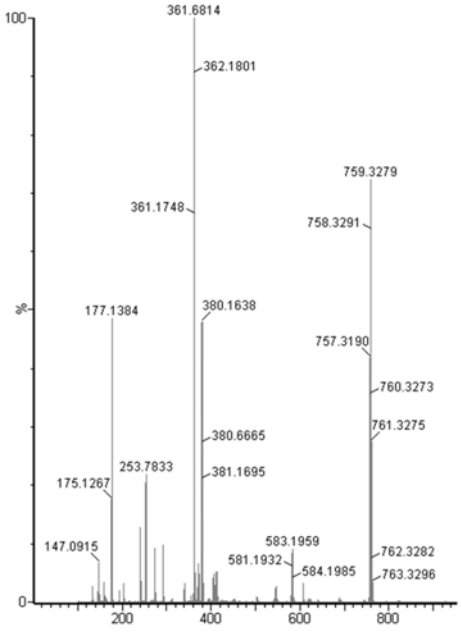

Figure S11. *ESI mass spectrum of* ***2b****.*

ESI-MS (2.8eV, positive mode, *m/z*): calcd for $[M]^+$ 759.3278; found 759.3279.

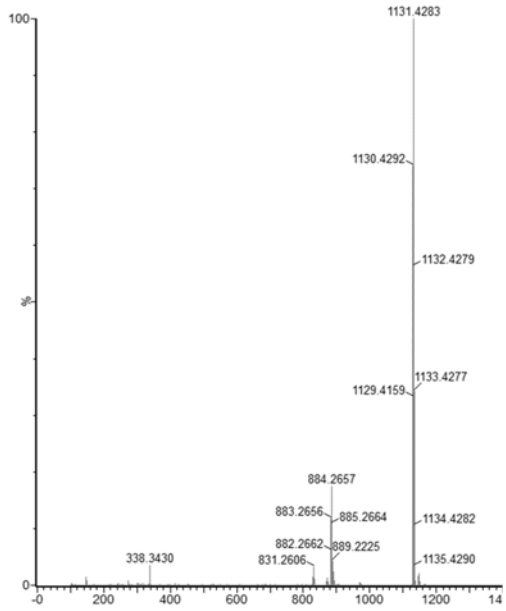

Figure S12. *ESI mass spectrum of* ***3b****.*

ESI-MS (2.8eV, positive mode, m/z): calcd for $[M]^+$ 1131.4262; found 1131.4283.

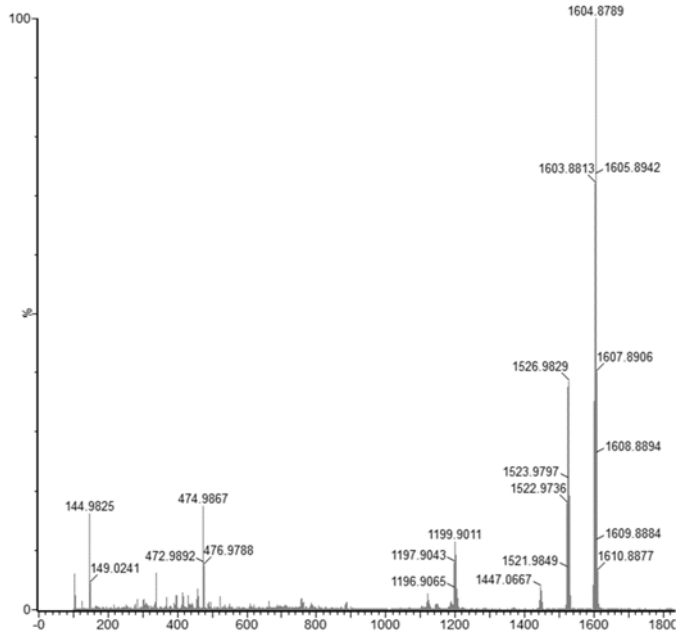

Figure S13. *ESI mass spectrum of* ***4b****.*

ESI-MS (2.8eV, positive mode, m/z): calcd for $[M\ ]^+$ = 1604.8787; found 1604.8789

Table S1. *High Resolution Mass spectrometry and Elemental Analysis*

Complex	Molecular Formula	MS(m/z)[a]		Elemental Analysis[a](%)		
		Fragment	Found(Calculated)	C	H	N
2a	$C_{22}H_{30}O_2N_2Cl_2Pt$	$[M+Na]^+$	643.1258 (643.1263)	-	-	-
3a	$C_{42}H_{38}O_2N_2Cl_2Pt$	$[M-Cl]^+$	833.2268 (833.2271)	64,38 (64,67)	5,15 (4,91)	3,81 (3,59)
4a	$C_{42}H_{34}O_2N_2Cl_2Br_2Pt$	$[M+Na]^+$	1206.8271 (1206.8236)	42,67 (42,59)	2,99 (2,89)	2,47 (2,37)
1b	$[C_{27}H_{33}N_3ClPt]^+$	$[M]^+$	630.2158 (630.2012)	-	-	-
2b	$[C_{33}H_{48}N_6ClPt]^+$	$[M]^+$	759.3278 (759.3279)	-	-	-
3b	$[C_{63}H_{60}N_6ClPt]^+$	$[M]^+$	1131.4283 (1131.4217)	64,62 (64,83)	4,94 (5,18)	7,58 (7,43)
4b	$[C_{63}H_{54}N_6Br_6ClPt]^+$	$[M]^+$	1604,8789 (1604,8786)	46,01 (46,12)	3,34 (3,32)	5,35 (5,13)

[a]found values are followed by calculated values in brackets

X-Ray Crystallography

Supporting Information available: Crystallographic data have been deposited with the Cambridge Crystallographic Data Centre as supplementary publication CCDC-1917581 for **2a**, CCDC-1917582 for **2b(I)**, and CCDC-1917583 for **2b(II)**. These data can be obtained free of charge via www.ccdc.cam.ac.uk/data_request/cif, or by emailing data request@ccdc.cam.ac.uk, or by contacting The Cambridge Crystallographic Data Centre, 12 Union Road, Cambridge CB2 1EZ, UK; fax: +44 1223 336033.

The intensity data for compounds **2a**, **2b(I)** and **2b(II)** were collected on a Nonius KappaCCD diffractometer at 133 K using graphite-monochromated Mo-*K*α radiation (λ = 0.71073Å). Data were corrected for Lorentz and polarization effects; absorption was considered on a semi-empirical basis using multiple-scans.[3–5] The crystal of **2a** was a non-merohedral twin. The twin law was determined by *PLATON*[6] to be (0.003 0.997 0.000) (1.003 -0.003 0.000) (0.000 0.000 -1.000). The contribution of the main component was refined to 0.845(1).The structures were solved by direct methods using *SHELXS*[7] and refined by full-matrix least squares techniques against Fo^2 using *SHELXL-97*.[8]

Table S2. *Crystal data and refinement details for the X-ray structure determinations.*

Compound	**2a**	**2b(I)**	**2b(II)**
Formula	$C_{22}H_{30}Cl_2N_2O_2Pt$	$C_{38}H_{46}Cl_2N_6O_5PtW$	$C_{33}H_{48}ClF_6N_6PPt$
fw ($g \cdot mol^{-1}$)	620.47	1116.65	904.28
T (K)	133(2)	133(2)	133(2)
crystal system	Triclinic	Orthorhombic	Orthorhombic
space group	P$\bar{1}$	*Pbcm*	*Pbca*
a (Å)	9.9173(6)	14.3993(2)	19.0522(4)
b (Å)	10.6646(7)	12.6163(2)	16.1120(3)
c (Å)	13.0011(9)	23.1624(4)	24.1876(4)
α (°)	90.386(4)	90	90
β (°)	108.898(3)	90	90
γ (°)	115.969(3)	90	90
V ($Å^3$)	1151.60(13)	4207.82(11)	7424.8(2)
Z	2	4	8
ρ ($g \cdot cm^{-3}$)	1.789	1.763	1.618
μ (mm^{-1})	6.345	6.227	3.957
measured data	14463	29406	45889
unique data / R_{int}	5213/0.0549	4928/0.0607	8435/0.0704
data with $I > 2\sigma(I)$	4568	4434	6798
R_1 (all data) [a]	0.0925	0.0388	0.0523
R_1 ($I > 2\sigma(I)$) [a]	0.0777	0.0319	0.0356
wR_2 (all data) [a]	0.1936	0.0684	0.0637
wR_2 ($I > 2\sigma(I)$) [a]	0.1838	0.0655	0.0588
S [b]	1.178	1.131	1.081
Resid. density ($e \cdot Å^{-3}$)	6.097/-2.048	0.975/-1.135	0.596/-0.513
absorpt. Method	multi-scan	multi-scan	multi-scan
absorpt. corr. $T_{min}/_{max}$	0.5225/0.7456	0.5686/0.7456	0.6580/0.7456
CCDC No.	1917581	1917582	1917583

[a] Definition of the *R* indices: $R_1 = (\Sigma \left|\left| F_o \right| - \left| F_c \right|\right|)/\Sigma \left| F_o \right|$;
$wR_2 = \{\Sigma[w(F_o^2-F_c^2)^2]/\Sigma[w(F_o^2)^2]\}^{1/2}$ with $w^{-1} = \sigma^2(F_o^2) + (aP)^2+bP$; $P = [2F_c^2 + Max(F_o^2,0)]/3$.

[b] Goodness of Fit: $S = \{\Sigma w(F_o^2-F_c^2)^2/(N_{ref}-N_{param})\}^{1/2}$.

Solid-state structure of 2a

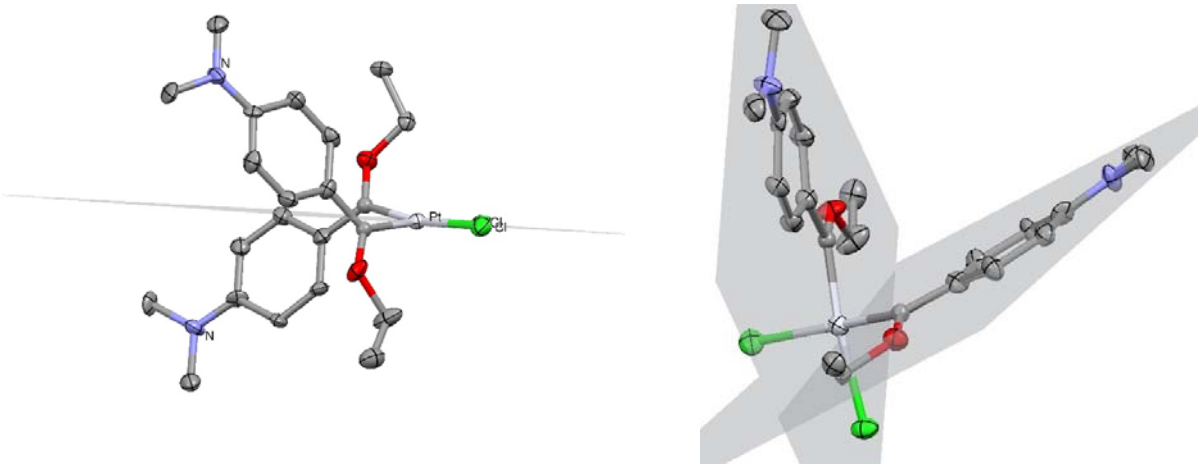

Figure S14. *Solid state structure representation* ***2a*** *viewed through the Pt(II) metal and chloro ligands* ***(left)*** *and the phenyl rings on the carbene ligands* ***(right)****.*

Complex **2a** crystallizes in space group $P\bar{1}$ with the two carbene ligands bonded to the Pt(II) metal centre in a *cis*-configuration to form a slightly distorted square planar complex. By constructing a plane through the Pt centre, a slight distortion of the square planar complex is observed with each carbene carbon lying slightly above or below the plane. A plane through the Pt atom and two carbene carbons adopts an angle of 12.72° relative to the plane through the Pt and two chloro ligands. Similarly, this indicates that the carbene carbons lie slightly out of the Pt(II) coordination plane. The coordination of the carbene ligands are arranged such that the ethoxy and phenyl substituents of the carbene carbons are found on opposite sides of the same plane.

This planarity is an indication of the conjugation that exists from the remote nitrogen, through the aromatic ring, to the carbene carbon for each of the ligands present in the complex. Further examination reveals that each carbene ligand, including its ethoxy group and the dimethylamino substituent lie in the plane of the phenylene ring. This is not the case for the precursor, the tungsten pentacarbonyl carbene complex (**2a**). The two planes through the carbene ligands form angles of 71.13 and 65.28° with the Pt(II) coordination plane.

Solid-state structures of 2b(I) and 2b(II)

Two crystal structures were obtained for **2b**, one with a $[W(CO)_5Cl]^-$ and the other with a PF_6^- counter ion and will be referred to as **2b(I)** and **2(II),** respectively. The bright yellow, rod-like crystals

were obtained by the slow diffusion of hexane into saturated dichloromethane solution of the corresponding complex.

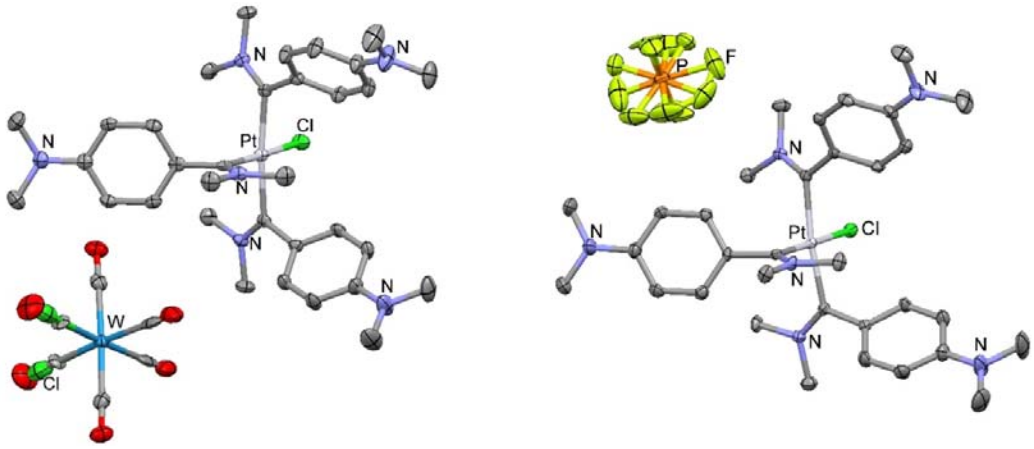

Figure S15. *Solid-state structures of* ***2b(I)*** *(left) and* ***2b(II)*** *(right). Ellipsoids are set at 50% probability; hydrogen atoms are omitted for clarity.*

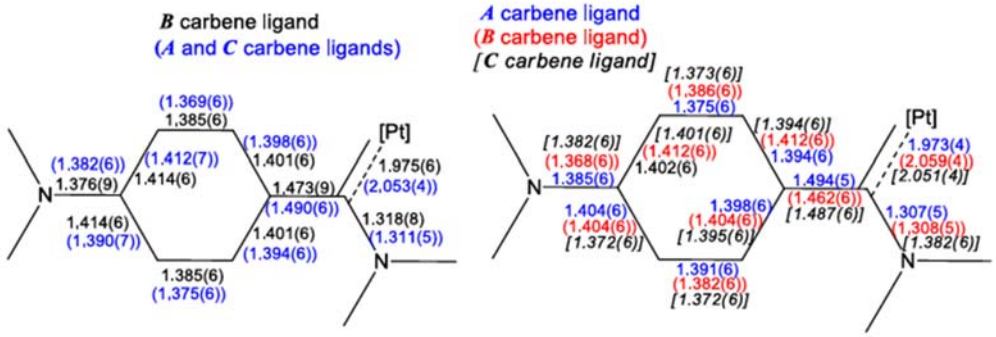

Figure S16. *Selected bond lengths (Å) of* ***2b(I)*** *and* ***2b(II)****.*

Three carbene ligands are coordinated to the square planar Pt(II) centre in both **2b(I)** and **2b(II)**. The fourth position, occupied by a chloro ligand, is crowded by the surrounding carbene ligands. There are no significant differences between the two single crystal structures except for the different counter ions. The counter ion for each complex is disordered in both structures. In **2b(I)**, the counter ion can lie in any position relative to the positively charged Pt(II) carbene complex, thus the average structure is displayed and for **2b(I)** in which the chlorine atom is orientated in one of two positions relative to the large Pt(II) complex. Therefore two of the counter ion bonds in the $[W(CO)_5Cl]^-$ anion is represented by both a W–CO bond and a W–Cl bond.

Packing patterns of 2a, 2b(I) and 2b(II)

The packing of **2a** along the three different axes is shown in Figure S17. The packing pattern is established by hydrogen bonding between the two chloro ligands and two protons of one carbene ligand. The unit motif is clearly shown along the *a*-axis. A Pt and one of its carbene ligands display intermolecular interaction with a second Pt and carbene ligand in a head to tail fashion. Hydrogen bonding between a chloro ligand and hydrogen atoms of methyl groups of both dimethyl amino substituents range from 2.78 – 2.91 Å (2.783, 2.916, 2.896 and 2.912 Å). The second chloro ligand interacts with a phenylene proton which is α to the NMe_2 substituent of the same carbene ligand (PtCl---H(Bz) = 2.778 Å). The same interactions apply for the other Pt centre and its chloro ligands. The packing pattern within the unit cell of **2a** displays the formation of separate layers, each consisting of a single molecule, while each layer expands through the alternate π-stacking of the flat dimethylamine aromatic rings of complexes in two different rows of the Pt(II) complexes as shown in

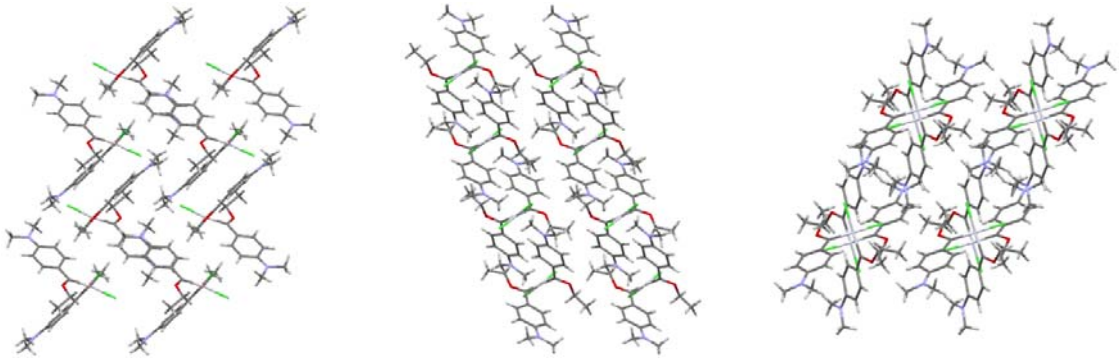

Figure S17. *Packing of molecules of* ***2a*** *along the a-, b- and c-axes (from left to right).*

The packing along the *b*-axis shows rows, each a single Pt complex thick. The packing along the *c*-axis again clearly shows formation of layers. The metal centres of the individual complexes are not aligned in a straight line, but rather arranged in a zig-zag fashion. The chloro ligands of adjacent complex molecules point in opposite directions. This allows for the OEt and NMe_2 groups to sufficiently far apart from each other such as not to cause repulsion between the groups.

Although **2b(I)** and **2b(II)** are essentially the same compounds, the exchange of the counter-ion remarkably influences the packing of the molecules axes (see S18). Complex **2b(I)** crystallises in space group *Pbcm* with a cell volume of 4207.82 Å^3, while **2b(II)** crystallises in space group *Pbca* with a unit cell volume of 7424.84 Å^3. The packing of the complexes themselves illustrate the intricacy of the networks and the symmetry and beauty of the packing patterns observed along different axes (S18, S19). In **2b(I)** the shortest hydrogen bonding contacts are between the carbonyl oxygens and protons of methyl groups of both amino substituents in carbene ligands and hydrogen of the benzene moiety (*ortho* to the carbene substituent). The packing patterns are determined by the counter ion $[W(CO)_5Cl]^-$ and the H-bonding interactions. Three different carbonyl oxygens of a $[W(CO)_5Cl]^-$ show interactions with three hydrogens on one carbene ligand, i.e, unlike for the chloro ligands of the biscarbene complex **2a**, the chloro ligand in **2b(I)** is shielded by the three bulky carbene ligands.

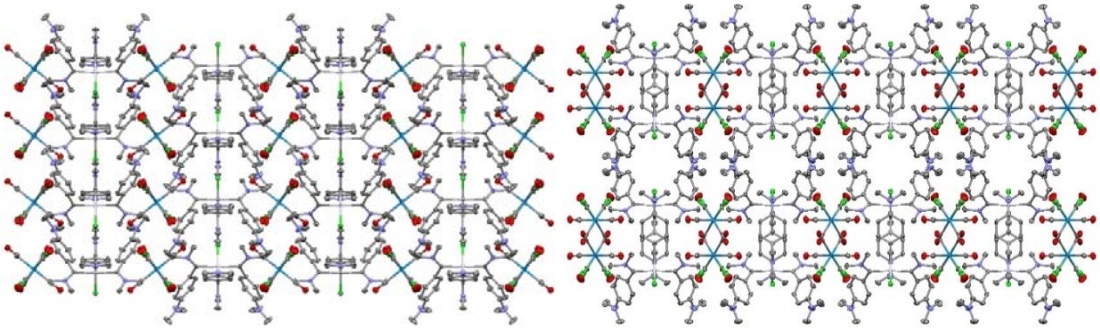

Figure S18. *Packing of* ***2b(I)*** *along the a-axis (left) and b-axis (right).*

In Figure *S*19 the packing of **2b(I)** is illustrated which shows the Pt–Cl bonds all lying in the same direction within a column, but each alternate column, separated by a $[W(CO)_5Cl]^-$ counter ion, has the Pt–Cl bond lying in opposite directions (Figure S18, left). By looking down the column (Figure S18, right), the staggering of each complex between the rings can be observed. Distinct tunnels throughout the complex are formed between the chloro ligands of two complexes and their carbene ligands' dimethylaniline substituents.

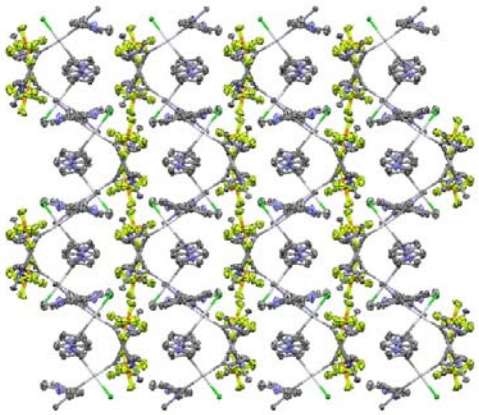

Figure S19. *Packing of* ***2b(II)*** *along the c-axis*

A clear pattern forms within the crystal lattice of **2b(II)** which can be viewed along its c-axis (S19) and takes the form of parallel sigmoidal curves. Hydrogen bonding between the chloro ligand and hydrogen atoms of methyl groups of both dimethyl amino substituents are in the range 2.78 – 2.91 Å (2.783, 2.916, 2.896 and 2.912 Å). This type of interaction was present in **2a** but not in **2b(I)**. Numerous F---H interactions in the range 2.45 – 2.65 Å are present between F atoms of the PF_6^- counter ion hydrogens of the methyl groups of the distant NMe_2 substituent and hydrogens of the benzene ring (α distant NMe_2 substituent).

Pt···Pt interactions

In the Pt(II) *tris*carbene complexes the carbene ligands are too bulky to allow form close contacts between the Pt ions of adjacent complex molecules. The intermolecular distances between Pt(II) metal centres are the smallest for **2a** with a distance of 6.210 Å and are even longer for the other complexes and rules out meaningful Pt----Pt interactions in the solid state.[9,10] The most prominent contribution to the packing in the crystal structure is the π–π interactions between aromatic groups of the carbene ligands in **2b(I)** and **2b(II)**.

Cyclic Voltammetry

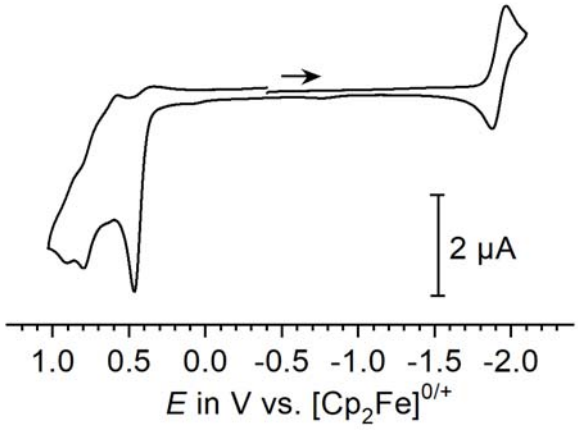

Figure S20 *Cyclic voltammogram over the full potential range of complex* ***[W{C(OEt)C$_6$H$_4$-4-NPh$_2$}(CO)$_5$]*** *(CH$_2$Cl$_2$ / NBu$_4$PF$_6$ (0.1 M)).*

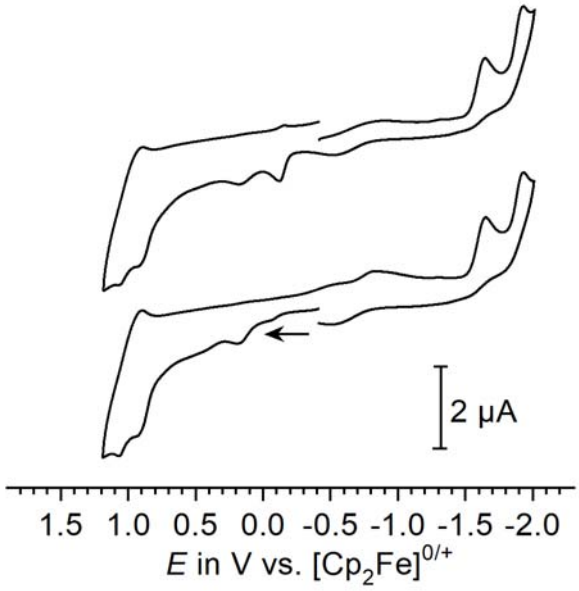

Figure S21. *Cyclic voltammograms of complex* ***2a*** *in CH$_2$Cl$_2$ / NBu$_4$PF$_6$ (0.1 M) at v = 0.1 V/s. Upper curve: cathodic scan first; lower curve: anodic scan first.*

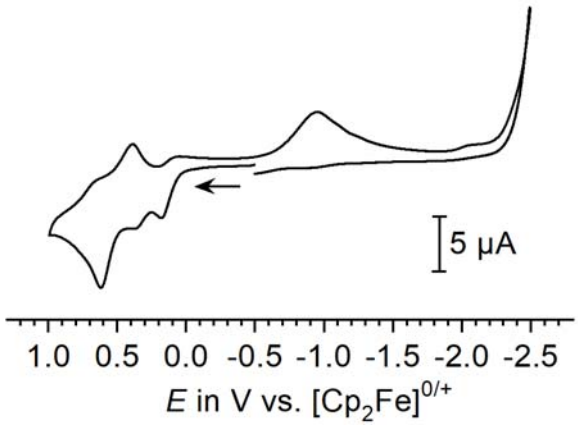

Figure S22. *Cyclic voltammograms of complex* ***2b*** *in CH_2Cl_2 / NBu_4PF_6 (0.1 M) at v = 0.1 V/s.*

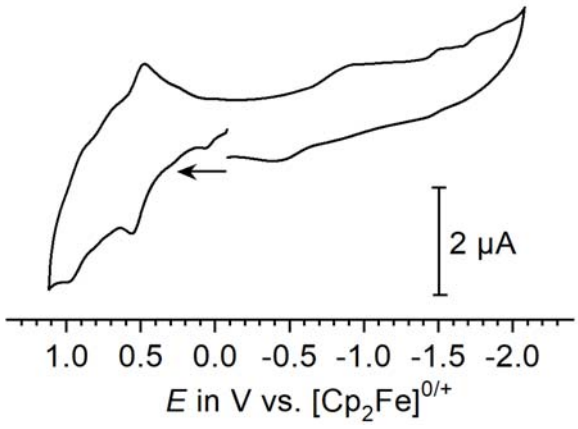

Figure S23. *Cyclic voltammograms of complex* ***3a*** *in CH_2Cl_2 / NBu_4PF_6 (0.1 M) at v = 0.1 V/s.*

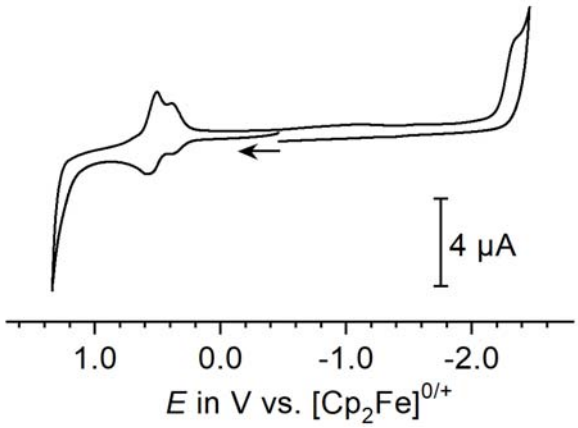

Figure S24. *Cyclic voltammograms of complex* ***3b*** *in CH_2Cl_2 / NBu_4PF_6 (0.1 M) at v = 0.1 V/s.*

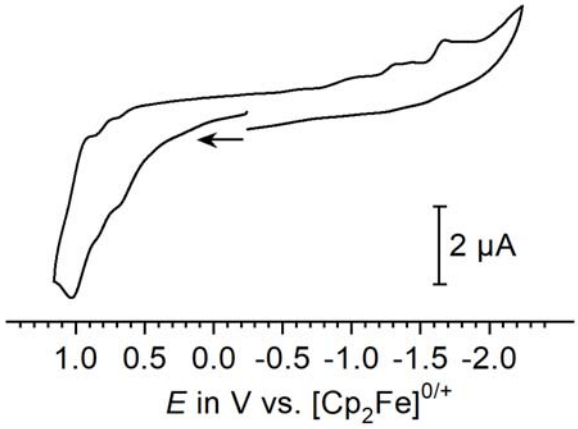

Figure S25. *Cyclic voltammograms of complex* ***4a*** *in CH_2Cl_2 / NBu_4PF_6 (0.1 M) at v = 0.1 V/s.*

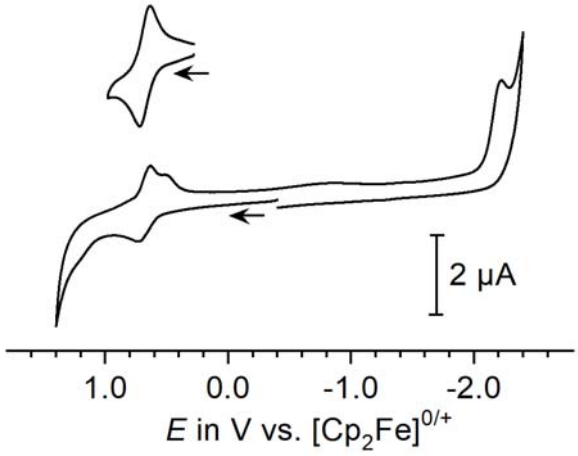

Figure S26. *Cyclic voltammograms of complex* ***4b*** *in CH_2Cl_2 / NBu_4PF_6 (0.1 M) at v = 0.1 V/s.*

References

[1] L. Rivera-Rivera, F. Colón-Padilla, A. Del Toro-Novalés, J.E. Cortés-Figueroa, Photosynthesis of (dihapto-buckminsterfullerene) pentacarbonyl tungsten (O), *J. Coord. Chem.* 54 (2001) 143–151.

[2] E.W. Abel, I.S. Butler, J.G. Reid, The anionic halogenopentacarbonyls of chromium, molybdenum, and tungsten, *J. Chem. Soc.* (1963) 2065–2068.

[3] R.W.W. Hooft, Collect Software, Nonius B.V., (1998).

[4] Z. Otwinowski, W. Minor, Processing of X-ray diffraction data collected in oscillation mode, *Methods Enzymol.* 276 (1997) 307–326.

[5] SADBS 2.10. Bruker-AXS inc., (2002).

[6] A.L. Spek, PLATON SQUEEZE: A tool for the calculation of the disordered solvent contribution to the calculated structure factors, *Acta Crystallogr. Sect. C*. 71 (2015) 9–18.

[7] G.M. Sheldrick, A short history of SHELX, *Acta Crystallogr. Sect. A*. 64 (2008) 112–122.

[8] G.M. Sheldrick, SHELXT - Integrated space-group and crystal-structure determination, *Acta Crystallogr. Sect. A*. 71 (2015) 3–8.

[9] S. Delahaye, C. Loosli, S.X. Liu, S. Decurtins, G. Labat, A. Neels, A. Loosli, T.R. Ward, A. Hauser, Inter- And intramolecular interactions in some supramolecular photochemical systems, *Adv. Funct. Mater.* 16 (2006) 286–295.

[10] S.W. Lai, M.C.W. Chan, T.C. Cheung, S.M. Peng, C.M. Che, Probing d8-d8 interactions in luminescent mono- and binuclear cyclometalated platinum(II) complexes of 6-phenyl-2,2′-bipyridines, *Inorg. Chem.* 38 (1999) 4046–4055.